POLITECNICO DI TORINO
Repository ISTITUZIONALE

Linearized Navier-Stokes equations as acoustic propagation model

Original
Linearized Navier-Stokes equations as acoustic propagation model / Lario, A., Arina, R.. - CD-ROM. - Proceedings of 22nd International Congress on Sound and Vibration 2015 (ICSV 22):(2015). (22nd International Congress on Sound and Vibration, ICSV 2015 ita 2015).

Availability:
This version is available at: 11583/2648929 since: 2023-07-01T09:18:44Z

Publisher:
International Institute of Acoustics and Vibrations

Published
DOI:

Terms of use:

This article is made available under terms and conditions as specified in the corresponding bibliographic description in the repository

Publisher copyright

(Article begins on next page)

15 November 2026

Florence, Italy 12-16 July 2015
ICSV22
The 22nd International Congress on Sound and Vibration

LINEARIZED NAVIER-STOKES EQUATIONS AS ACOUSTIC PROPAGATION MODEL

Andrea Lario and Renzo Arina
Dipartimento di Ingegneria Meccanica e Aerospaziale
Politecnico di Torino, corso Duca degli Abruzzi 24, I-10129 Torino, Italy
email: renzo.arina@polito.it

An acoustical model based on the Linearized Navier-Stokes (LNS) equations is proposed. The inclusion of the viscous terms enables to represent hydrodynamic-acoustic interactions responsible of the generation of vorticity associated with hydrodynamic modes. The LNS equations are solved with a high-order accurate and low-dispersive numerical scheme. Time integration is performed using a fourth-order, six-stage Runge-Kutta scheme which has low dispersion and dissipation errors, the space discretization is based on a Discontinuous Galerkin formulation on unstructured grids and sponge-layer boundary conditions are introduced to avoid spurious wave reflections. The model is applied to the analysis of the acoustic propagation of an incoming perturbation inside a circular duct with a sudden area expansion in presence of a mean flow . At corners, the acoustic oscillations are strongly affected by viscous effects, vortical perturbations are generated at the wall and convected into the duct by the mean flow field. The computed coefficients of the scattering matrix are compared with experimental data for a convective Mach number equal to 0.29.

1. Introduction

In the case of acoustic propagation in complex geometries with a mean flow, significant hydrodynamic-acoustic interactions, coupling acoustic waves and vortical modes, may occur. For example in ducts with sudden changes of area, where flow separation may be present in correspondence of sharp edges, with a consequent generation of vorticity due to viscous effects. To correctly capture this coupling, the mechanisms responsible of the generation of vorticity associated with the hydrodynamic modes must be included in the model. The Linearized Euler Equations (LEE) model both the acoustic propagation as well as the vorticity transport. However some ambiguities remains on the vorticity generation process which is ultimately due to the viscous effects. The inclusion of the viscous terms not only solve the problem of a correct generation of vorticity, but may also contribute to solve the problem of representing the Kelvin-Helmholtz instabilities, connected with the propagation of the vortical modes, which make the current LEE models highly unstable. The explicit inclusion of the viscous terms removes the need of adding artificial viscosity or to resort to other fictitious mechanisms to stabilize the numerical solution of the LEE. The linearized Navier-Stokes (LNS) equations can be a valid alternative to the LEE model for acoustic propagation problems.

The objective of the present work is to include the viscous effects into the acoustic wave propagation model obtained linearizing the Navier-Stokes equations, for a compressible flow, with respect to

a representative mean flow. In this work an efficient numerical algorithm for the solution of the LNS equations is proposed. To our knowledge, there are only few works dealing with the solution of the LNS for aeroacoustics, and mainly in the frequency domain [1]. The present method solves the LNS equations in the time domain on unstructured grids.

The occurrence of geometrical complexities, such as sharp edges, where acoustic energy is transferred into the vortical modes for viscous effects, requires an highly accurate numerical scheme with not only reduced dispersive properties, to accurate model the wave propagation, but also providing a very low level of numerical dissipation on unstructured grids. The Discontinuous Galerkin Method (DGM) is one of the most appropriate numerical scheme satisfying these requirements. The DGM displays many interesting properties: it is compact, regardless of the order of the element, data are only exchanged between neighboring elements. It is well suited for complex geometries because it can be applied to an unstructured grid, even non conformal. The expected dispersion and dissipation properties are retained also on unstructured grids. One of the disadvantages of the DGM is its computational cost. Because of the discontinuous character, there are extra degrees of freedom at cell boundaries in comparison to the continuous finite elements, demanding more computational resources. This drawback can be partially reduced with a parallel implementation of the algorithm, an operation which is not too difficult because of the compactness property of the scheme. Another disadvantage is the need of quadrature for the weighted residual formulation, but it can be eliminated by adopting a quadrature-free approach [2]. Considering only elements with constant Jacobian, i.e. with a linear mapping to the reference element (elements with straight edges), all integrals can be evaluated during the initialization step. The time discretization is based on a low dissipation formulation of a fourth-order accurate Runge-Kutta scheme [3]. Explicit time integration, the more appropriate for acoustic wave propagation, avoids inversion of a large algebraic system and it is well suited for parallel computation. Along numerical boundaries, to avoid incoming spurious reflections, a sponge-layer boundary condition is used [4].

The paper is organized as follows. In Section 2, the LNS equations are presented for general coordinates and for axisymmetric problems, The DGM formulation for the LNS equations is described in Section 3, as well as the time integration algorithm and the non-reflecting boundary conditions. In Section 4 the evaluation of the scattering matrix for a sudden area discontinuity in a cylindrical duct in presence of mean flow is reported. The numerical results are validated using experimental data of Ronneberger [5].

2. Linearized Navier-Stokes equations

2.1 General coordinate formulation

Denoting with $(.)_0$ the mean flow variables, and with $(.)'$ the acoustic perturbations, the governing equations for a general coordinate system read

$$\frac{\partial \mathbf{q}}{\partial t} + \nabla\cdot \mathbf{F}^c = \nabla\cdot \mathbf{F}^d + \mathbf{g} + \mathbf{h} \quad , \tag{1}$$

where $\mathbf{q} = [\rho', \rho_0\mathbf{v}', p']^T$ is the acoustic vector. $\mathbf{F}^c$ and $\mathbf{F}^d$ are the convective and viscous fluxes, defined as follows

$$\mathbf{F}^c = \begin{pmatrix} \rho_0\mathbf{v}' + \rho'\mathbf{v}_0 \\ \rho_0\mathbf{v}_0\mathbf{v}' + p'\mathbf{I} \\ \gamma p_0\mathbf{v}' + p'\mathbf{v}_0 \end{pmatrix} \quad , \quad \mathbf{F}^d = \begin{pmatrix} 0 \\ \boldsymbol{\tau}' \\ (\gamma-1)\kappa\nabla\cdot T' \end{pmatrix} \quad ,$$

γ is the specific heat ratio for a perfect gas and κ the thermal conductivity coefficient. The viscous stresses $\boldsymbol{\tau}'$, being μ the dynamic viscosity coefficient and μ_B the bulk viscosity coefficient, are linearly related to the velocity fluctuation gradients

$$\boldsymbol{\tau}' = \mu\left[(\nabla\mathbf{v}' + \nabla\mathbf{v}'^T) - \frac{2}{3}(\nabla\cdot\mathbf{v}')\mathbf{I}\right] + \mu_B(\nabla\cdot\mathbf{v}')\mathbf{I} \quad .$$

The bulk viscosity term can be neglected because it affects the acoustic propagation only over extremely long distances, when the accumulation of its influence over each cycle becomes important and eventually dissipate the acoustic perturbation.

The vector $\mathbf{g}$, containing the zero-th order terms and the mean flow derivatives, reads

$$\mathbf{g} = \begin{pmatrix} 0 \\ -\rho' \left(\frac{\partial \mathbf{v}_0}{\partial t} + \mathbf{v}_0 \cdot \nabla \mathbf{v}_0\right) - \rho_0 \mathbf{v}' \cdot \nabla \mathbf{v}_0 \\ (\gamma - 1)\left(\mathbf{v}' \cdot \nabla p_0 - p' \nabla \cdot \mathbf{v}_0\right) + (\gamma - 1)\left[(\boldsymbol{\tau}_0 \cdot \nabla) \cdot \mathbf{v}' + (\boldsymbol{\tau}' \cdot \nabla) \cdot \mathbf{v}_0\right] \end{pmatrix} .$$

The source vector $\mathbf{h}$ contains explicit source terms, like a mass source or a force source.

LNS equations can be simplified assuming an isentropic relation between pressure and density fluctuations. This assumption is not valid if an explicit addition of heat is present, such as in combustion processes, or if heat conduction is not negligible; but it is applicable to non reacting problems at low Mach number. In this case pressure and density are related by the relation $p' = c_0^2 \rho'$ where $c_0^2 = \gamma p_0 / \rho_0$ is the velocity of sound. With this assumption one dependent variable is removed from the system and therefore the energy equation can be omitted from the system (1).

The LEE equations can be obtained from the (1) simply dropping out the viscous fluxes $\mathbf{F}^d$ and setting to zero $\boldsymbol{\tau}'$ and $\boldsymbol{\tau}_0$ in the expression of $\mathbf{g}$.

2.2 Axisymmetric formulation

For axisymmetric problems, it is convenient to rewrite the governing equations in a cylindrical coordinate system, namely (r, θ, z). If both the geometry and the mean flow can be assumed axisymmetric, i.e.,

$$v_{0\theta} = 0\,, \quad \frac{\partial}{\partial \theta}\left[(.)_0\right] = 0\,, \quad \frac{\partial}{\partial \theta}\left[(.)'\right] = 0\,,$$

where $v_{0\theta}$ is the θ-component of the mean flow velocity, the LNS equations can be written in cylindrical coordinates as

$$\frac{\partial \mathbf{u}}{\partial t} + \frac{1}{r}\frac{\partial \mathbf{F}_r^c}{\partial r} + \frac{\partial \mathbf{F}_z^c}{\partial z} = \frac{1}{r}\frac{\partial \mathbf{F}_r^d}{\partial r} + \frac{\partial \mathbf{F}_z^d}{\partial z} + \mathbf{f}_p + \mathbf{g}_{axy} + \mathbf{h}\,, \tag{2}$$

where $\mathbf{u} = [\rho',\, \rho_0 v_r',\, \rho_0 v_z',\, p']^T$ is the acoustic perturbation vector. Here $(v_r',\, v_z',)$ are the velocity components in (r, z) directions respectively. $\mathbf{F}_r^c$ and $\mathbf{F}_z^c$ contain part of the inviscid fluxes, the pressure gradient term being contained into $\mathbf{f}_p$, and $\mathbf{F}_r^d$ and $\mathbf{F}_z^d$ the viscous fluxes along r and z directions respectively:

$$\mathbf{F}_r^c = \begin{pmatrix} \rho' v_{0r} + \rho_0 v_r' \\ \rho_0 v_{0r} v_r' \\ \rho_0 v_{0r} v_z' \\ r\left(\gamma p_0 v_r' + p_\prime v_{0r}\right) \end{pmatrix}, \quad \mathbf{F}_r^d = \begin{pmatrix} 0 \\ r\tau_{rr}' \\ r\tau_{rz}' \\ (\gamma - 1)\kappa r \frac{\partial T'}{\partial r} \end{pmatrix},$$

$$\mathbf{F}_z^c = \begin{pmatrix} \rho' v_{0z} + \rho_0 v_z' \\ \rho_0 v_{0z} v_r' \\ \rho_0 v_{0z} v_z' \\ \gamma p_0 v_z' + p_\prime v_{0z} \end{pmatrix}, \quad \mathbf{F}_z^d = \begin{pmatrix} 0 \\ \tau_{rz}' \\ \tau_{zz}' \\ (\gamma - 1)\kappa \frac{\partial T'}{\partial z} \end{pmatrix},$$

and

$$\mathbf{f}_p = -\left[0, \frac{\partial p'}{\partial r}, \frac{\partial p'}{\partial z}, 0\right]^T$$

The vector $\mathbf{g}_{axy}$ contains terms of the mean flow due to axi-symmetry and the mean flow derivatives and $\mathbf{h}$ represents the acoustic sources,

$$\mathbf{g}_{axy} = \begin{pmatrix} 0 \\ -\left[\rho' \frac{\partial v_{0r}}{\partial t} + (\rho' v_{0r} + \rho_0 v_r') \frac{\partial v_{0r}}{\partial r} + (\rho' v_{0z} + \rho_0 v_z') \frac{\partial v_{0r}}{\partial z}\right] \\ -\left[\rho' \frac{\partial v_{0z}}{\partial t} + (\rho' v_{0r} + \rho_0 v_r') \frac{\partial v_{0z}}{\partial r} + (\rho' v_{0z} + \rho_0 v_z') \frac{\partial v_{0z}}{\partial z}\right] \\ (\gamma - 1) g_{axy}^z \end{pmatrix} .$$

where

$$\begin{aligned} g_{axy}^z &= \left(v_{0r}\frac{\partial p'}{\partial r} + v_{0z}\frac{\partial p'}{\partial z}\right) + \left(v_r'\frac{\partial p_0}{\partial r} + v_z'\frac{\partial p_0}{\partial z}\right) + \\ &\left(\frac{\tau_{0rr}}{r}\frac{\partial}{\partial r}(r v_r') + \tau_{0rz}\frac{\partial v_r'}{\partial z}\right) + \left(\frac{\tau_{0rz}}{r}\frac{\partial}{\partial r}(r v_z') + \tau_{0zz}\frac{\partial v_z'}{\partial z}\right) + \\ &\left(\frac{\tau_{rr}'}{r}\frac{\partial}{\partial r}(r v_{0r}) + \tau_{rz}'\frac{\partial v_{0r}}{\partial z}\right) + \left(\frac{\tau_{rz}'}{r}\frac{\partial}{\partial r}(r v_{0z}) + \tau_{zz}'\frac{\partial v_{0z}}{\partial z}\right) \quad , \end{aligned}$$

and

$$\begin{aligned} \tau_{rr}' &= 2\mu\frac{\partial v_r'}{\partial r} + \left(\mu_B - \frac{2}{3}\mu\right)\left[\frac{1}{r}\frac{\partial}{\partial r}(r v_r') + \frac{\partial v'}{\partial z}\right] \quad , \\ \tau_{rz}' &= \mu\left(\frac{\partial v_r'}{\partial z} + \frac{\partial v_z'}{\partial r}\right) \quad , \\ \tau_{zz}' &= 2\mu\frac{\partial v_z'}{\partial z} + \left(\mu_B - \frac{2}{3}\mu\right)\left[\frac{1}{r}\frac{\partial}{\partial r}(r v_r') + \frac{\partial v'}{\partial z}\right] \quad . \end{aligned}$$

3. DGM-RK numerical method

3.1 Spatial dicretization

LNS equations (1) define a linear convection-diffusion problem over the domain $\Omega \subset \mathcal{R}^3$, which can be cast in the form

$$\frac{\partial \mathbf{u}}{\partial t} + \nabla \cdot (\mathbf{F}^c(\mathbf{u}) + \mathbf{F}^d(\mathbf{u}, \nabla\mathbf{u})) + \mathbf{g} = \mathbf{h} \qquad \text{in } \Omega \, , \tag{3}$$

where $\mathbf{u}$ is the m-dimensional vector of the unknowns, $\mathbf{F}^c$ are the convective fluxes, $\mathbf{F}^d$ are the diffusive fluxes, $\mathbf{g}$ is the source term and $\mathbf{h}$ is the forcing term.

To apply the Discontinuous Galerkin formulation, the domain Ω must be partitioned into a collection of disjointed elements K named $\mathcal{T}_h$. The faces of the elements in the collection defines the set $\partial\mathcal{T}_h := \{\partial K : K \in \mathcal{T}_h\}$. On each element K, a finite element space is introduced for $\mathbf{u}$

$$\mathbf{W}_h^k = \left\{\mathbf{w} \in \left(L^2(\mathcal{T}_h)\right)^m : \mathbf{w}|_K \in \left(\mathcal{P}^k(K)\right)^m \ , \forall\, K \in \mathcal{T}_h\right\} \, ,$$

where $\mathcal{P}^k(D)$ denotes the space of polynomials of degree at most k on a domain D and $L^2(\mathcal{D})$ is the space of square integrable functions on D. Applying the Galerkin projection method to each element, it is possible to find an approximate solution to $\mathbf{u}$ in the finite element space $\mathbf{W}_h$. On each element, the variational problem becomes: find an approximation $\mathbf{u}_h \in \mathbf{W}_h^k$ such that for all $K \in \mathcal{T}_h$

$$\begin{aligned} &\left(\frac{\partial \mathbf{u}_h}{\partial t}, \mathbf{w}\right)_K - \left(\mathbf{F}^c(\mathbf{u}_h) + \mathbf{F}^d(\mathbf{u}_h), \nabla\mathbf{w}\right)_K + \\ &\qquad + \left\langle \left(\widehat{\mathbf{F}}_h^c + \widehat{\mathbf{F}}_h^d\right)\cdot\mathbf{n}, \mathbf{w}\right\rangle_{\partial K} + (\mathbf{g}, \mathbf{w})_K = (\mathbf{h}, \mathbf{w})_K \, , \qquad \forall\, \mathbf{w} \in \left(\mathcal{P}^k\right)^m \, , \end{aligned} \tag{4}$$

The numerical fluxes $\widehat{\mathbf{F}}_h^c$ and $\widehat{\mathbf{F}}_h^d$ are an approximation of $\mathbf{F}^c(\mathbf{u})$ and $\mathbf{F}^d(\mathbf{u})$ over ∂K respectively, expressed in the following form

$$(\widehat{\mathbf{F}}_h^c + \widehat{\mathbf{F}}_h^d)\cdot\mathbf{n} = (\mathbf{F}^c(\widehat{\mathbf{u}}_h) + \mathbf{F}^d(\widehat{\mathbf{u}}_h)\cdot\mathbf{n} + \mathbf{S}(\mathbf{u}_h,\widehat{\mathbf{u}}_h)(\mathbf{u}_h - \widehat{\mathbf{u}}_h)\ , \qquad \text{on } \partial K\ , \tag{5}$$

where $\widehat{\mathbf{u}}_h$ is an approximation to the trace of the solution $\mathbf{u}$ on ∂K and it is single-valued over each edge. $\mathbf{S}(\mathbf{u}_h,\widehat{\mathbf{u}}_h)$ is a local stabilization matrix.

The assembled problem is obtained by adding the contributions (4) over all the elements and enforcing the continuity of the normal component of the numerical fluxes

$$\left\langle \left(\widehat{\mathbf{F}}_h^c + \widehat{\mathbf{F}}_h^d\right)\cdot\mathbf{n}, \mu\right\rangle_{\partial\mathcal{T}_h\setminus\partial\Omega} + \left\langle \widehat{\mathbf{B}}_h, \mu\right\rangle_{\partial\Omega} = 0 \qquad \forall\mu\in\mathbf{M}_h^k\ , \tag{6}$$

where $\widehat{\mathbf{B}}_h$ is the numerical flux vector of dimension m and is defined over the boundary $\partial\Omega$.

Equation (6) enforces the continuity of the normal component of the numerical flux, which can be interpreted point-wise over the interior faces as a jump condition. Inserting the definition of the numerical fluxes (5) it follows, with $[\![.]\!]$ defining the jump across the interface,

$$[\![\left(\mathbf{F}^c(\widehat{\mathbf{u}}_h) + \mathbf{F}^d(\widehat{\mathbf{u}}_h,\mathbf{q}_h)\right)\cdot\mathbf{n}]\!] + \mathbf{S}^+\mathbf{u}_h^+ + \mathbf{S}^-\mathbf{u}_h^- - (\mathbf{S}^+ + \mathbf{S}^-)\widehat{\mathbf{u}}_h = 0\ ,$$

where $(.)^{\pm}$ denote the traces of the quantity $(.)$ on the interior faces between two neighboring elements. Since $\mathbf{S}$ is constant over a face, i.e. $\mathbf{S} = \mathbf{S}^+ = \mathbf{S}^-$, the auxiliary variable $\widehat{\mathbf{u}}_h$ can be expressed on the interior faces as

$$\widehat{\mathbf{u}}_h = \frac{1}{2}\mathbf{S}^{-1}[\![\left(\mathbf{F}^c(\widehat{\mathbf{u}}_h) + \mathbf{F}^d(\widehat{\mathbf{u}}_h,\mathbf{q}_h)\right)\cdot\mathbf{n}]\!] + \frac{1}{2}\left(\mathbf{u}_h^+ + \mathbf{u}_h^-\right)\ .$$

The stabilization matrix $\mathbf{S}$ is chosen using the local Lax-Friedrichs splitting, and is given by the expression $\mathbf{S} = \lambda_{\max}\mathbf{I}$, where λ_{max} is the maximum absolute value of the eigenvalues of the local Jacobian matrix $[\partial\mathbf{F}^c(\widehat{\mathbf{u}}_h)/\partial\widehat{\mathbf{u}}_h]\cdot\mathbf{n}$, and $\mathbf{I}$ is the identity matrix. With this stability matrix the numerical fluxes become

$$\begin{aligned}
\widehat{\mathbf{u}}_h &= \frac{1}{2\lambda_{\max}}[\![\left(\mathbf{F}^c(\widehat{\mathbf{u}}_h) + \mathbf{F}^d(\widehat{\mathbf{u}}_h)\right)\cdot\mathbf{n}]\!] + \frac{1}{2}\left(\mathbf{u}_h^+ + \mathbf{u}_h^-\right)\ ,\\
(\widehat{\mathbf{F}}_h^c + \widehat{\mathbf{F}}_h^d)\cdot\mathbf{n} &= \left(\mathbf{F}^c(\widehat{\mathbf{u}}_h) + \mathbf{F}^d(\widehat{\mathbf{u}}_h)\right)\cdot\mathbf{n} + \lambda_{\max}\left(\mathbf{u}_h^+ - \mathbf{u}_h^-\right)\ , \qquad \text{on } \partial K\ .
\end{aligned}$$

3.2 Time integration

Time integration is performed using a fourth-order, six-stage Runge-Kutta scheme which has low dispersion and dissipation errors [3]. Classical third- and fourth-order Runge-Kutta schemes provide relatively large stability limits but, for acoustic calculations, the stability consideration alone is not sufficient, since the Runge-Kutta schemes retain both dissipation and dispersion errors. Instead of choosing the coefficients of the Runge-Kutta scheme to optimize the maximum order of accuracy, it is possible to select coefficients so as to minimize the dissipation and the dispersion errors. Moreover, this optimization does not introduce additional stability constraints and sufficiently large time steps can be used, which therefore increase the efficiency of the computation. The Runge Kutta scheme is implemented using the low-storage Willamson's formulation, which only requires two storage locations per variable.

3.3 Boundary conditions

To avoid spurious reflections along numerical boundaries, sponge layers are added to the computational domain. In the current formulation, sponge layers act both damping the solution and applying a virtual stretch to the computational mesh.

The damping[4] is applied multiplying the solution by a damping function ζ which gradually decreases from 1 to 0. The function ζ is defined as

$$\zeta = (1 - C_1 x_l^2) \left(1 - \frac{1 - e^{C_2 x_l^2}}{1 - e^{C_2}} \right) ,$$

where $C_1 = 0$ and $C_2 = 13$. The quantity x_l is the normalized distance from the inner border of the sponge layer. Thus x_l ranges from 0 to 1, marking, respectively, the beginning and the end of the sponge layer. The virtual stretching [6] has the effect to gradually slow down waves in the layer, this can be achieved with a coordinate transformation. Along a layer, the transformation $x = x(\xi)$ is defined as the backward solution from the virtually stretched coordinate $\xi = [\xi_1, \xi_2]$, with ξ_1 and ξ_2 being the starting and the ending coordinates of the virtually stretched layer, of the ordinary differential equation

$$\frac{d}{d\xi}(x) = \eta(x(\xi), \xi) \qquad x(\xi_2) = x_2 ,$$

where x_2 is the ending coordinate of the physical layer. The stretching function $\eta(x)$ can be chosen as $\eta = 1 - (1 - \varepsilon_l)[1 - (1 - x_l)^p]^q$, where $p = 3.25$, $q = 1.75$ and $\varepsilon_l = 10^{-4}$.

The combination of the two strategies leads to an efficient approach that requires shorter buffer layers and is computationally efficient.

Walls are assumed impermeable and acoustically rigid, this means that no flow passes through the boundary and that acoustic waves are totally reflected. Two different boundary conditions can be imposed at the walls: slip or no-slip boundary condition. The slip flow boundary condition forces the velocity to be tangent to the wall, which can be evaluated at timestep $j + 1$ from the values at the previous timestep as

$$(\mathbf{u}_w)^{j+1} = (\mathbf{u}_w)^j - \left[(\mathbf{u}_w)^j \cdot \mathbf{n} \right] \mathbf{n} .$$

The pressure fluctuations at the wall are evaluated linearizing the exact solution of the Riemann problem for a reflective wall

$$(p_w)^{j+1} = (p_w)^j + p_0 \frac{\gamma}{c_0} (u_w)^j .$$

For the LNS equations an additional boundary condition should be imposed on the temperature.

4. Cylindrical duct with sudden area expansion

As test case the calculation of the acoustic propagation of an incoming perturbation inside a circular duct with a sudden area expansion in presence of a mean flow is shown. At the corner, the acoustic oscillations are strongly affected by viscous effects, vorticity is generated and convected into the duct by the mean flow field. No analytical method is able to predict the coefficients of the scattering matrix of such acoustic network with a satisfying level of accuracy, especially for mean flows characterized by Mach numbers greater than 0.1 [7]. Therefore the development of an accurate computational model for this kind of problems is of great practical interest. Experimental data have been provided by Ronneberger [5] for several mean flow Mach numbers. The measurements were performed on a cylindrical area discontinuity with an upstream diameter $h_1 = 50$ mm and a downstream diameter $h_2 = 85$ mm, corresponding to an area ratio equal to $\eta = 0.346$.

In the computational domain, the length of the upstream and downstream ducts are $l_1 = 1.5$ m and $l_2 = 2.75$ m respectively. Since the acoustic field is axisymmetric, only half of the domain is considered. The LNS equations are solved using elements of degree $p = 4$. To absorb the outgoing wave and avoid spurious reflections, two sponge layers with a thickness of 0.75 m are placed at the inflow and outflow boundaries. The mean flow field in the duct has been calculated solving the steady-state incompressible Reynolds-averaged Navier-Stokes (RANS) equations with a $k - \omega$ model. The inlet turbulent length scale is set equal to 1 mm and the turbulent intensity to 10%, fixed

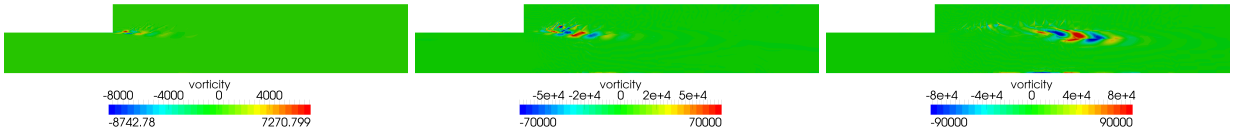


Figure 1: Instantaneous vorticity fluctuations [1/s] at for $M_0 = 0.29$ from left to right: t=$4.0\,10^{-3}$ s, t=$4.8\,10^{-3}$ s, t=$5.6\,10^{-3}$ s.

ambient pressure boundary condition at the outlet boundary and prescribed velocity profile at inlet are imposed.

In the frequency-domain calculations [1, 8] the acoustic source is modeled as a sinusoidal function with a specified frequency. With the time-domain approach the monochromatic wave can be substituted with time domain wave packet. This approach, suitable for linear problem, replace the monochromatic sinusoidal source with a single temporally compact broadband pulse. Such a wave packet contains a broad range of frequencies in a short time duration and it is possible to solve with one computation all frequencies within numerical resolution. Details of the wave packet technique can be found in [9].

Considering the case with mean flow Mach number $M_0 = 0.29$, the effect of the mean flow can be seen in figure 1, where the instantaneous vorticity perturbation is plotted for three different times.

The relationship between the transmission and the reflection of incoming sound waves through an acoustics element can be described using the scattering-matrix formalism. A general network element can be thought of as a black box to which acoustic waves enter and exit through the so-called ports. For a two-port element, without active processes, the scattering-matrix formalism could be written as

$$\begin{pmatrix} p_{a-} \\ p_{b+} \end{pmatrix} = \overbrace{\begin{pmatrix} R^+ & T^- \\ T^+ & R^- \end{pmatrix}}^{S} \begin{pmatrix} p_{a+} \\ p_{b-} \end{pmatrix} \quad ,$$

where a and b represent the inflow and outflow ports respectively and p_+ and p_- are the Fourier coefficients of the transmitted and reflected acoustics waves. The matrix $\boldsymbol{S}$ is the scattering matrix and takes into account the passive transmission and reflection of sound waves. To evaluate the scattering matrix $\boldsymbol{S}$ the two source-location method is applied: first the problem is solved with a time-harmonic

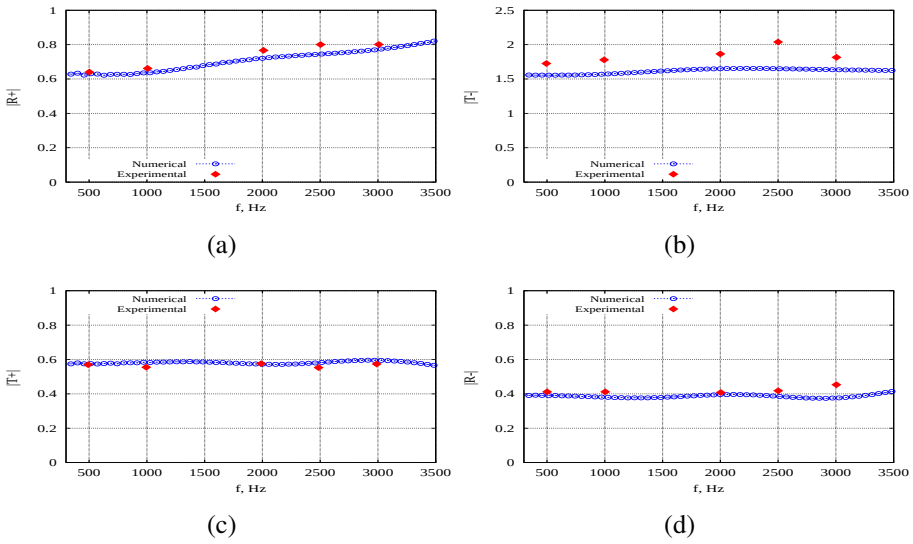


Figure 2: Amplitude of the scattering matrix terms with an inlet Mach number $M = 0.29$. Circles (◯): numerical, diamonds (⋄): experiments. (a) $|R+|$; (b) $|T-|$; (c) $|T+|$; (d) $|R-|$.

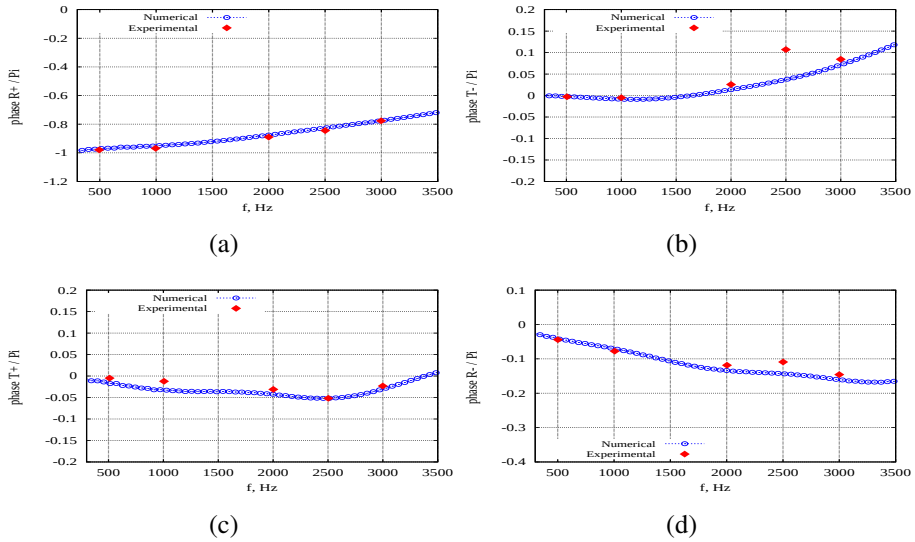


Figure 3: Phase of the scattering matrix terms with an inlet Mach number $M = 0.29$. Circles (◯): numerical, diamonds (⋄): experiments. (a) $\phi(R+)/\pi$; (b) $\phi(T-)/\pi$; (c) $\phi(T+)/\pi$; (d) $\phi(R-)/\pi$.

wave entering from the inflow, and then the problem is solved with the same wave entering from the outflow port [9]. The scattering coefficients, compared with the experimental ones [5], are reported in figures 2 and 3.

REFERENCES

1. Kierkegaard, A., Boij, S. and Efraimsson, G. A frequency domain linearized Navier-Stokes Equations Approach to Acoustic Propagation in Flow Ducts with Sharp Edges, *The Journal of the Acoustical Society of America*, **127** (2), 710–719, (2010).

2. Atkins, H. L. Quadrature-free Implementation of the Discontinuous Galerkin Method for Hyperbolic Equations, *AIAA Journal*, **36** (5), 775–782, (1998).

3. Berland, J., Bogey, C. and Bailly, C. Low-dissipation and Low-dispersion Fourth-order Runge-Kutta Algorithm, *Journal of Computational physics*, **35**, (2006).

4. Richards, S. K., Zhang, X., Chen., X. X. and Nelson, P. A. The Evaluation of Non-reflecting Boundary Conditions for Duct Acoustic Computation, *Journal of Sound and Vibration*, **270**, 539–557, (2004).

5. Ronneberger, D. Theoretical and experimental investigations of sound propagation in flow ducts with area expansion and perforated plates, DFG-Abschlussbericht, Universititat Gottingen, (1987).

6. Appelö, D. and Colonius, T. A High-order Super-grid-scale Absorbing Layer and Its Application to Linear Hyperbolic Systems, *Journal of Computational Physics*, **228**, 4200–4217, (2009).

7. Boij, S. and Nilsson, B. Scattering and Absorption of Sound at Flow Duct Expansions, *Journal of Sound an Vibration*, **289** (3), 995–1004, (2006).

8. Na, W., Efraimsson, G. and Boij, S. Simulations of the Scattering of Sound Waves at a Sudden Area Expansion in a 3D Duct, *Proceedings of the 21th International Congress on Sound and Vibration*, Beijing, China, 13–17 July, (2014).

9. Lario, A., Arina, R. and Iob, A. A Discontinuous Galerkin Method for the Solution of the Linearized Navier-Stokes Equations, *19th AIAA/CEAS Aeroacoustics Conference; Berlin, Germany*, AIAA Paper 2013-2168, (2013).